Second Harmonic Generation as a Probe of Multisite Adsorption at Solid−Liquid Interfaces of Aqueous Colloid Suspensions†

ARTICLE *in* THE JOURNAL OF PHYSICAL CHEMISTRY C · MARCH 2007

Impact Factor: 4.77 · DOI: 10.1021/jp061730h

Second Harmonic Generation as a Probe of Multisite Adsorption at Solid−Liquid Interfaces of Aqueous Colloid Suspensions†

R. Kramer Campen,‡,§ De-sheng Zheng,|| Hong-fei Wang,|| and Eric Borguet*,§

Department of Geosciences, Pennsylvania State University, University Park, Pennsylvania 16802, State Key Laboratory of Molecular Reaction Dynamics, Institute of Chemistry, Chinese Academy of Sciences, Beijing, China, 100080, and Department of Chemistry, Temple University, Philadelphia, Pennsylvania 19122

Received: March 20, 2006; In Final Form: August 9, 2006

Chemistry at the surface of solid particles in colloidal dispersions is important in the description of such diverse topics as nutrient and contaminant flow in the environment and the creation of better paints and cosmetics. Particles in these systems are often characterized by molecular-level, surface heterogeneity. This molecular heterogeneity influences many aspects of the chemical processes of interest, among the simplest of which is physisorption. In this study we construct adsorption isotherms for the triphenylmethane dye Malachite Green on various latex particles using the flow through Second Harmonic Generation (ftSHG) technique. This technique makes it possible to construct significantly higher resolution isotherms than conventional separation methods. Here we chose both particles that we expect to be chemically homogeneous (plain polystyrene) and particles whose surface we expect to have molecular level heterogeneity (carboxylated and hydroxylated polystyrene). We find that, using the ftSHG isotherms, we are able to quantify the adsorption energies and site densities of multiple adsorption sites on the carboxylated and hydroxylated polystyrene particles but find only a single type of adsorption site on the plain polystyrene. We expect the ability to measure adsorption site energy and density on chemically heterogeneous latex colloids will be useful in the creation of better biosensors and that the application of ftSHG to other chemically heterogeneous colloids should provide insight into a variety of natural and engineered processes.

1. Introduction

Much of the chemistry that confers useful properties on the products we use, helps our body function effectively, and controls the quality of the environment in which we live is heterogeneous. Often this chemistry occurs at the surface of solid particles in colloidal dispersions. An understanding of the molecular mechanisms of adsorption and reaction at such particle surfaces should give insight into, for example, the stability of microorganisms in the marine water column, help in understanding the dispersion rates of contaminants in the groundwater of certain aquifers, and may aid in the development of better products: more stable paint and cosmetics and more efficient biosensors.[1−4]

Detailed chemical knowledge of these environments requires characterizing the number of adsorbates at the particle surface, their orientation or conformation and, if adsorption is specific, the functional group/functional group association by which it is mediated. Classical surface science techniques (such as XPS and TEM) typically involve the use of electrons or molecules as probes and are thus generally unsuitable for solid/liquid interfaces.[5] While often applied to measure adsorbate conformation at planar interfaces,[6] scanning probe techniques are difficult to apply to colloidal systems without first immobilizing the particles on some kind of surface, as is commonly done for particle size measurements.[7] Conventional (i.e. linear) spectroscopic measurements of adsorbed species typically require either difficult cancellation of a large bulk signal (e.g., H^1 NMR of water adsorbed on silica[8]), special sample geometry (e.g., attenuated total reflectance FTIR[9]), or are not generally applicable to all adsorbates on all types of particles (e.g., surface enhanced Raman[10]).

The simplest method of quantifying adsorption on solid surfaces in colloidal dispersions is through an adsorption isotherm. In principle, an adsorption isotherm reflects the details of interaction of an adsorbate with a surface: e.g., does an adsorbing molecule interact with the surface specifically or nonspecifically, if adsorption is specific is there one surface functional group engaged in interaction with the surface or many, do the adsorbates interact with each other, and does multilayer adsorption occur? Typically, this sort of plot is generated via a separation protocol: a series of samples of constant particle concentration, but with variable amounts of analyte, are created and allowed to interact. After interaction, the particles are separated from the sample (most often with either centrifugation or filtration) and the resulting depletion of the analyte in the remaining bulk solution is measured. This procedure is time-consuming and therefore such analyses are often restricted to a small number of samples.[11]

Understanding many adsorbate/colloid systems requires a knowledge of the number and relative energies of any adsorption sites present. For example,[12,13] understanding of the fate of Cu in groundwater hinges on the recognition that it adsorbs on clay minerals by three different mechanisms (each of which may be independently enhanced or suppressed with changes in pH, ionic strength, or competition from other adsorbates). In the past, the presence of discrete adsorption sites has often been determined

† Part of the special issue "Kenneth B. Eisenthal Festschrift".
* Address correspondence to this author.
‡ Pennsylvania State University.
§ Temple University.
|| Chinese Academy of Sciences.

10.1021/jp061730h CCC: $37.00
Published on Web 03/22/2007

by spectroscopic methods with relative adsorption energies calculated (from bulk thermodynamic quantities or direct molecular simulation of the surface). Often such measurements require relatively inaccessible equipment (synchrotron based X-ray absorption spectroscopies) or are relatively time-consuming (electronic structure calculations of surface systems containing several hundred atoms). In principle, the presence of multiple adsorption sites (although not their chemical identity) and the relative density and energy of these sites can be inferred from adsorption isotherms. If possible, such measurements would provide useful insight into relatively complex adsorption that is difficult to gain by other means. The application of adsorption isotherms in this manner has most often been limited by the relatively small number of measurements in the typical experiment: a sufficiently coarse sampling of the isotherm obscures subtle changes in curvature that may provide physical insight. The ability to quantitatively distinguish multiple and single site adsorption on particle surfaces in colloidal dispersions thus requires a method that can sensitively and rapidly make many measurements. Such a method could be extremely useful in the mechanistic understanding of virtually all molecular processes that occur at particle surfaces.

Second Harmonic Generation (SHG) is an interface specific second-order optical process[14,15] with sensitivity to <1% of a monolayer in many cases and general applicability to both equilibrium and dynamical properties at various planar interfaces.[16,17] Ten years ago the unambiguous application of SHG to adsorbates on aqueous colloids was demonstrated.[18] Since then SHG has been used to characterize adsorption at the surface of soft colloids,[19] on mineral colloids,[20] of dye molecules, surfactants, and polypeptides on latex,[21−23] as well as colloidal surface potential and charge density.[24] The automation of both SHG measurement and sample creation, using a flow through system (ftSHG),[21] has made it possible to create relatively high-resolution adsorption isotherms (i.e., more than 100 measurements) in a fraction of the time necessary to create a low-resolution isotherm (i.e., 5−10 measurements), using the separation protocol.

Latex microparticles are often used as in situ biosensors because of their relative ease of functionalization and large surface area.[25,26] To fully exploit these particles as scaffolds for subsequent sensor design it would be useful to have molecular level information on the number of functional groups at their surfaces. Polystyrene is relatively unreactive so particle biosensor synthesis is often done on functionalized latex particles that, in addition to surface phenyl groups, have some concentration of more reactive surface groups (e.g., carboxyl or amino).[27] Quantifying the amount and binding energies of each site would provide insight into more efficient strategies for sensor synthesis. High-resolution adsorption isotherms on such surfaces with an appropriate probe molecule should allow phenomenological insight into this problem.

Here we employ the triphenylmethane dye Malachite Green (MG) as a probe molecule to study surfaces of plain, carboxylated, and hydroxylated polystyrene latex particles, denoted PPS, cPPS, and hPPS, respectively, in an aqueous dispersion. MG is a useful probe molecule (see Figure 1) for these particle surfaces because at our experimental pH it is cationic as well as being relatively polarizable. The former characteristic implies that MG should experience significant electrostatic interaction with the surface, while the later allows the possibility for adsorption via van der Waals (vdW) interactions.

In this study we compare adsorption isotherms for this system generated using both separation and ftSHG methods. We find, in line with expectations, that the ftSHG isotherms (which typically have 10× more data points than the separation isotherms) allow us to quantitatively distinguish between the goodness of fit of different phenomenological surface models in a manner not often possible with other types of measurements. We also find, once again in line with expectations, that isotherms describing the adsorption of MG on cPPS and hPPS particles are better described by a two-site Langmuir, while isotherms describing adsorption on PPS particles are better described by a single site. Taken together, the separation and ftSHG experiments allow the determination of both surface site energies and absolute adsorbate densities.

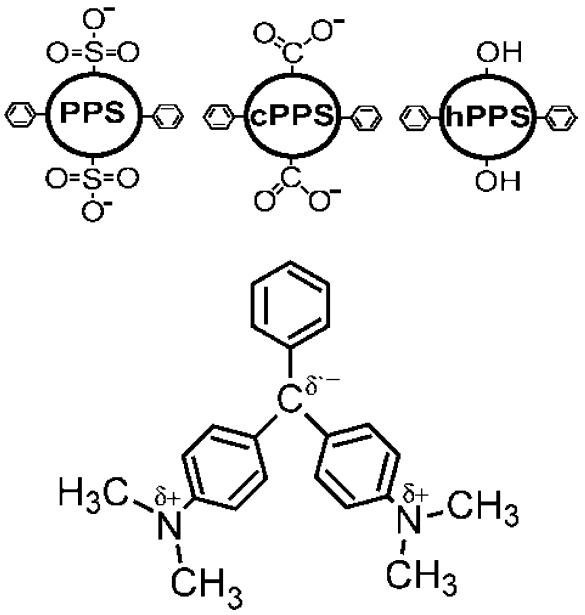

Figure 1. Structure of Malachite Green and schematic representation of particle surfaces at pH 3.

2. Methods

2.1. Experimental Details. PPS (1.053 μm diameter), cPPS (0.984 μm), and hPPS (0.915 μm) particles from Polysciences Inc (Polybead Polystyrene, Carboxylate and Hydroxylate Microspheres) were used as received. We expect the surfaces of PPS particles to expose a significant density of phenyl groups along with some small number of sulfonate groups, while cPPS and hPPS particles are expected to have significant concentrations of carboxyl/hydroxyl and phenyl and the same small concentration of sulfonate groups.[28] Malachite Green was purchased in its carbinol form from Sigma Aldrich and also used as received. Solutions were acidified with reagent grade concentrated HCl and Millipore 18.2 MΩ·cm grade water. All experiments were conducted at pH = 3. All glass and Teflon bottles used in making solutions were cleaned by boiling in SC1 (30% H_2O_2, NH_4OH, and H_2O (1:1:4)) for 30 min, while optical cuvettes used in the creation of UV−visible absorbance spectra were cleaned with piranha solution (to avoid possible cuvette etching in SC1).

Adsorption isotherms were generated by using a separation protocol for PPS, cPPS, and hPPS with the particle separation step accomplished via centrifugation. Samples with a particle concentration of 10^9 particles/mL were prepared in Teflon centrifuge tubes and centrifuged at 20 000 rpm for 15 min (relative centrifugal force = 36700*g*). Tests with these parameters suggested better than ∼90% particle removal efficiency.

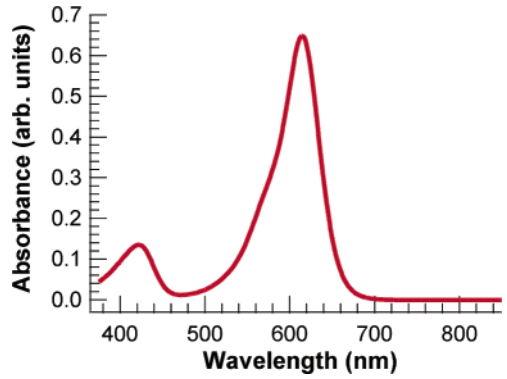

Figure 2. Absorbance spectrum of a 35 μmol solution of Malachite Green at pH 3.

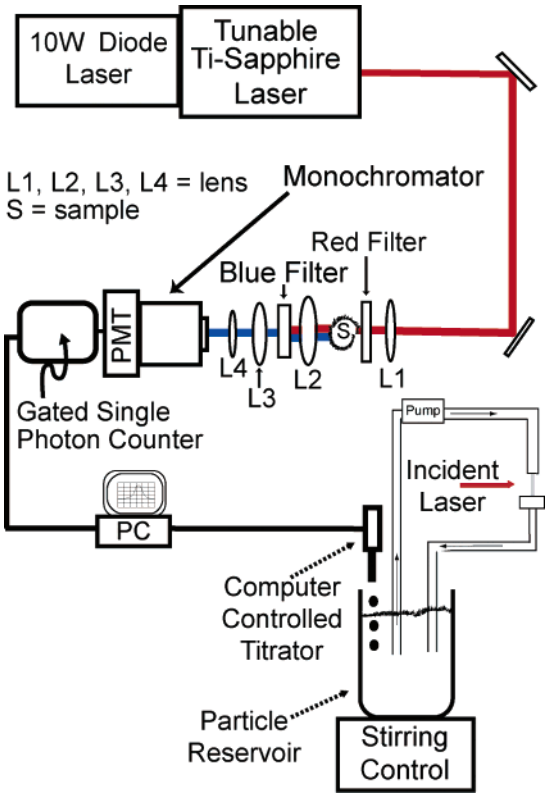

Figure 3. Schematic representation of flow through the SHG (ftSHG) experimental setup. Our setup is slightly modified from ref 19.

For the centrifuged samples, moles absorbed were quantified by using the measured absorbances (at 617 nm) of samples containing MG with and without particles, the particle surface area provided by Polysciences, and the experimentally determined absorption coefficient of MG at pH 3 and 617 nm. A 10 times larger concentration of particles in the separation protocol, compared to the ftSHG experiments, was required to detect a measurable change in optical absorbance.

To generate the SHG isotherms we used a system shown schematically in Figure 3. This apparatus has been described before,[21] so will be only briefly reviewed here: a broadband, tunable, mode-locked femtosecond Ti−sapphire laser system (Millennium Xs and Tsunami 3955, Spectra-Physics Inc) was used to generate 800 nm light. This light was focused onto the sample jet and filtered to remove second harmonic generated prior to the sample. After passing through the sample it was collimated, filtered to remove the incident beam, focused into a monochromator, and detected at 400 nm with a high gain photomultiplier tube (R585, Hamamatsu) and a photon counter (SR400, Stanford Research Systems). Laser power at the sample was 260 mW.

The sample delivery system was a particle reservoir (initial particle concentration was 10^8 particles/mL) connected, via Teflon tubing, to a metal nozzle just above the beam path, collected via a metal funnel below the beam path and returned to the reservoir. Sample was circulated through this loop with use of a peristaltic pump and MG was added to the particle reservoir with use of a computer controlled buret (CAT Contiburette). Over the course of experiments on PPS, cPPS, and hPPS the volume of fluid in the reservoir increased by less than 5%. Data analysis with and without volume correction indicated no difference between the two: results presented here are model fits to data without volume correction. For each data point collected in the experiment we counted for 20 s. After counting we added an additional aliquot of MG to the reservoir, waited 10 s for the system to equilibrate, and counted again.

2.2. Data Analysis. Measured SHG intensity (I_{SH}) from systems with interfacial adsorbates is known to depend on adsorbate number, orientation, hyperpolarizability, and bulk and interfacial refractive indices.[14,15,29] For our system the bulk refractive indices are similar at 400 and 800 nm (~1.55 for PS and 1.3 for water[30,31]) and the interfacial density of MG at surface saturation is low relative to systems (e.g., Langmuir−Blodgett monolayers) in which interfacial refractive index is known to vary as a function of surface density.[29] We therefore expect any changes in interfacial refractive index with adsorption to have a minor effect on our measured SH intensity. Our SH frequency (400 nm) is close to resonance with the MG electronic transition at 424 nm (see Figure 2). Prior work describing the adsorption of MG at the surface of oil droplets in water has shown no evidence for adsorption influencing the 424 nm transition.[32] We therefore follow prior workers [33] and argue that, over the MG concentration range and utilizing the 800 nm fundamental employed in this experiment, the molecular hyperpolarizability of MG is not likely to change as a function of surface coverage.

This leaves us with a measured quantity that responds both to the number of adsorbate molecules and their orientation. For planar interfaces it has been demonstrated that it is possible to choose a set of experimental conditions that ensure I_{SH} is relatively insensitive to orientation changes.[34−37] However, no such work has been done for colloidal interfaces. For the construction of adsorption isotherms it is of little importance whether MG absorbs in different orientations at different particle surfaces. To interpret our isotherms in the usual manner it is only necessary that MG orientation is not changing as a function of surface coverage. We can assess the likelihood of this scenario by examining the qualitative shapes of the measured ftSHG isotherms.

To zeroeth order we imagine three possible shapes for adsorption isotherms (see Figure 4). Option A is typically interpreted as indicating monolayer, Langmuir-like adsorption, option B as indicating multilayer adsorption, surface coverage induced rearrangement, or multisite adsorption with wide separation in site energies (e.g., this shape is commonly found in acid/base titrations of aqueous solutions of polyprotic acids or oxide surfaces[38]), and option C as possibly indicating competitive adsorption. If adsorption at our particle surface occurs as a monolayer we expect I_{SH} to increase with increasing initial concentration to some saturation value because of its dependence on the number of MG molecules adsorbed. If changes in orientation of adsorbed MG occur as a function of the number of MG molecules at the colloidal particle surface

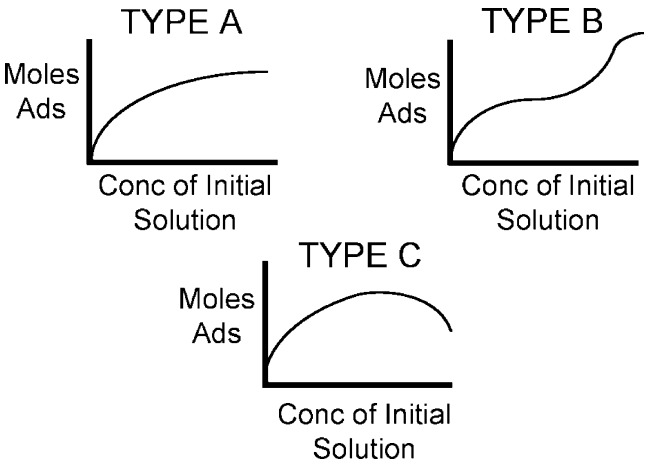

Figure 4. Classes of adsorption isotherm. Type A is typically taken to indicate monolayer adsorption. Type B is often interpreted as indicating multilayer adsorption, multisite adsorption with wide separation in site energies or adsorbate induced conformation change. Type C is more ambiguous but may indicate the presence of additional phases in solution or surface poisoning.

(MG_{surf}), and these changes act to enhance SHG per molecule, we would expect I_{SH} to be enhanced at sufficiently high initial concentration of MG, qualitatively similar to option B. If changes in molecular orientation at high MG_{surf} act to diminish SHG per molecule we expect a qualitative picture similar to option C. Only if changes in I_{SH} due to orientation are negative, and of precisely equal magnitude to those due to increasing MG_{surf}, would isotherm A result when changes in molecular orientation as a function of surface coverage are important. Because this scenario seems unlikely, and because our data were in general of type A, we believe it reasonable to interpret SHG isotherms that are similar to type A as being indicative of monolayer adsorption and resulting solely from increases in adsorbate number.

In the separation experiments, molecules adsorbed are measured directly so data were fit to expressions of the form

$$N = \theta N_m \tag{1}$$

where N = molecules adsorbed, N_m = maximum number of molecules adsorbed, and θ = fractional surface coverage. Following prior workers,[21] I_{SH} can be written

$$I_{SH} = I_{back} + (\alpha + \xi\theta e^{i\varphi})^2 \approx (\xi\theta)^2 \tag{2}$$

where I_{back} is the background contribution to the measurement, α is the nonresonant coherent contribution to the nonlinear polarization from water at the particle surface, ξ is the nonlinear polarization associated with full surface coverage of MG, θ is the surface coverage (a function of C, initial concentration), and φ is the phase relationship between the α and ξ components of the nonlinear polarization. Extensive testing suggested that the signal from aqueous solutions of MG and the signal from solutions containing bare particles were small relative to the signal from the surface bound MG species (<2% of maximum intensity). Furthermore, we saw no evidence for interference (no departures from $I_{SH} \propto (\xi\theta)^2$) between these two components at low MG concentration. For this reason we fit the SHG data using the simplification of eq 2 shown on the far right: we assumed I_{back} and α are zero.

To interpret the data requires a phenomenological surface model that relates the initial concentration of MG added to θ. As with any fitting of a model to data, a good fit does not prove that the model accurately captures the underlying phenomenon nor does it suggest that other models (i.e., beyond those tested) may not better describe the data. What a good fit does do is to demonstrate that, of the models tested, the better fitting one is a better description of the data. Data from all experiments were fit with three different surface models: a classical Langmuir model, a Langmuir model modified to allow for pairwise adsorbate interaction, and a two-site Langmuir model (the model assumptions, parameters, and references are described in Table 1). For reasons discussed at some length below, we argue that the three models chosen are likely the simplest models that might possibly describe the data. Two versions of each model were employed, one of which assumed that the number of MG molecules adsorbed was much less than the number remaining in solution ($[MG_{bulk}] \gg [MG_{surf}]$), and a generalized version that did not make this assumption. This results in a total of six attempted model fits for each experiment. It is important to note that in the case of $[MG_{bulk}] \gg [MG_{surf}]$ each generalized model reduces to its simplified version so any additional parameters available in the generalized model (see Table 1) cannot be determined with accuracy in the limit of small bulk concentration depletion. For example, the maximum number of surface sites (N_m) does not appear in the classical Langmuir model but does in the generalized Langmuir (Lang and gLang in Table 1). If the gLang model is fit to an experimental system in which $MG_{surf} \ll MG_{bulk}$, the N_m resulting from the model fit to the data will be inaccurate.

To quantify the differences in goodness of fit between different models fit to the same experimental data the reduced chi squared (χ^2_{red}) of each fit was calculated.[39] In the limit of infinitely many data points with perfectly known error, and if the chosen model correctly describes the data, the χ^2_{red} would be 1. The closer to this limit, either with respect to number of measurements or knowledge of error, the greater should be the ability to distinguish quantitatively between different surface models. On average each ftSHG isotherm contained ~10× more measurements than the separation experiments. Clearly these larger data sets should allow knowledge of χ^2_{red} with much greater precision for each attempted model fit and hence a much enhanced ability to quantitatively distinguish appropriate models.

In our initial attempts at data analysis we observed some dependence of model parameter(s) on initial guess(s). We addressed this problem by testing model solutions to 5 000−10 000 initial guesses (varying each model parameter over 4−5 orders of magnitude) and using those which produced the lowest χ^2_{red}. All fitting was performed with the analysis and visualization software Igor Pro (Wavemetrics). For each minimization we employed this program's standard implementation of the Marquadt−Levenberg algorithm. Two examples of the results of this process, best fits to one of the ftSHG cPPS, and one of the ftSHG PPS experiments are shown in Figure 5.

To calculate a χ^2_{red} for each model/experimental data pair an estimate of error for each measurement is required. For the ftSHG data we used the standard deviation associated with photon counting for this purpose. In most cases this counting error is likely an underestimate: there is likely some contribution to the error from sample preparation. For experiments on planar interfaces it is relatively easy to estimate the total error (sample preparation, counting, optical alignment, laser intensity, etc.) by comparing the signal from a sample to that of a relatively stable reference (often a quartz crystal). Unfortunately, suspensions of particles scatter light in a different manner than either crystals or bulk liquids, thus either of these media is, at best, a mediocre reference.[40] We made some attempts to check our

TABLE 1: Surface Adsorption Models[a]

model type	assumptions	equation	ref
Langmuir (Lang)	1. no adsorbate interaction 2. single adsorption site 3. monolayer adsorption 4. $[MG_{bulk}] \gg [MG_{surf}]$	$\theta = \left(\frac{\frac{K_{eq}C}{55.5}}{1+\frac{K_{eq}C}{55.5}}\right)$	44
generalized Lang (gLang)	1. no adsorbate interaction 2. single adsorption site 3. monolayer adsorption	$\theta = \frac{\left(C+N_m+\frac{55.5}{K_{eq}}\right)-\sqrt{\left(C+N_m+\frac{55.5}{K_{eq}}\right)^2-4CN_m}}{2N_m}$	41
interacting Langmuir (iLang)	1. *adsorbate interaction* (*dimer*) 2. single adsorption site 3. monolayer adsorption 4. $[MG_{bulk}] \gg [MG_{surf}]$	$\theta = \left(\frac{\frac{K_{eq}C}{55.5}}{1+\frac{K_{eq}C}{55.5}}\right)+2K_i\left(\frac{\frac{K_{eq}C}{55.5}}{1+\frac{K_{eq}C}{55.5}}\right)^2 N_m$	this work
generalized interacting Langmuir (giLang)	1. *adsorbate interaction* (*dimer*) 2. single adsorption site 3. monolayer adsorption	$\theta = \frac{\left(C+N_m+\frac{55.5}{K_{eq}}\right)-\sqrt{\left(C+N_m+\frac{55.5}{K_{eq}}\right)^2-4CN_m}}{2N_m}+\left[\left(C+N_m+\frac{55.5}{K_{eq}}\right)-\sqrt{\left(C+N_m+\frac{55.5}{K_{eq}}\right)^2-4CN_m}\right]^2\frac{K_i}{2N_m}$	this work
two-site Langmuir (2Lang)	1. no adsorbate interaction 2. *two adsorption sites* 3. monolayer adsorption 4. $[MG_{bulk}] \gg [MG_{surf}]$	$\theta = \left(\frac{N_{mA}}{N_{mA}+N_{mB}}\right)\left(\frac{\frac{K_{eqA}C}{55.5}}{1+\frac{K_{eqA}C}{55.5}}\right)+\left(\frac{N_{mB}}{N_{mA}+N_{mB}}\right)\left(\frac{\frac{K_{eqB}C}{55.5}}{1+\frac{K_{eqB}C}{55.5}}\right)$	45
generalized two-site Langmuir (g2Lang)	1. no adsorbate interaction 2. *two adsorption sites* 3. monolayer adsorption	$\theta = \left(\frac{\left(C+N_{mA}+\frac{55.5}{K_{eqA}}\right)-\sqrt{\left(C+N_{mA}+\frac{55.5}{K_{eqA}}\right)^2-4CN_{mA}}}{2}+\frac{CK_{eqB}N_{mB}-N_{mA}N_{mB}K_B-\frac{55.5K_{eqB}N_{mB}}{K_{eqA}}+K_{eqB}N_{mB}\sqrt{\left(C+N_{mA}+\frac{55.5}{K_{eqA}}\right)^2-4CN_{mA}}}{111+CK_{eqB}-N_{mA}K_B-\frac{55.5K_{eqB}}{K_{eqA}}+K_{eqB}\sqrt{\left(C+N_{mA}+\frac{55.5}{K_{eqA}}\right)^2-4CN_{mA}}}\right)(N_{mA}+N_{mB})^{-1}$	this work

[a] Mathematical forms of the surface adsorption models, and the assumptions involved in their derivation. The generalized two-site model we employed allows an arbitrary relationship between $[MG_{bulk}]$ and $[MG_{surf}]$ with respect to only one of the surface sites. The variables employed in the equations are as follows: θ = fractional surface coverage, C = initial bulk concentration of MG, K_{eq} = equilibrium constant of adsorption, K_{eqA} = equilibrium constant of adsorption with respect to site A, K_{eqB} = equilibrium constant of adsorption with respect to site B, K_i = equilibrium constant with respect to surface interaction, N_m = maximum moles of adsorbed MG per unit volume, N_{mA} = maximum number of adsorbed moles of MG at site A per unit volume, and N_{mB} = maximum number of adsorbed moles of MG at site B per unit volume (for two-site models $N_{mA} + N_{mB} = N_m$). C is the independent variable in all fits.

measurements vs the SH signal in our setup from bulk water but have no expectation that this is an ideal reference. We expect, therefore, that our SH error will be underestimated and that, as a result, the χ^2_{red} will be too high. However, as we are principally interested in the best model description of data for a given experiment, and we expect this additional error to be random, every model fit is expected to overestimate χ^2_{red} in a similar manner and this problem seems unlikely to be significant. We estimated the error for each point in the separation experiments on the basis of replicate measurements.

To summarize, we analyzed our data as follows: for each experiment we applied each of the six models, for each model attempting 5 000−10 000 different initial guesses. Next, for each model we chose the initial parameters that produced the lowest χ^2_{red}. This gave us six possible solutions (one for each model) for each experiment. Attempts to fit a particular model to replicate experiments of MG adsorbed on the same particle type would produce the same χ^2_{red} (if we knew the error accurately and had the same number of data points for each experiment). We thus averaged the χ^2_{red} for the fit of each model type to each replicate experiment. The model that produced the lowest average value of χ^2_{red} over replicate experiments on a given particle type was taken to be the best (see Table 2).

Having chosen the best fitting model, the next step is to evaluate that model's parameters. We calculated our best guess for a model parameter, in fitting data to a particular experiment, by averaging all values of that parameter for solutions within 0.001 of the minimum in χ^2_{red}. We then averaged the value for the given parameter attained from fitting to replicate experiments on the same system. These results are reported in Tables 3 and 4. This approach is equivalent to assuming that all fits of a given model to a particular system (e.g., all fits of the two-site Langmuir model to the cPPS experiments) were equally good. We analyzed parameter uncertainty in this manner because our use of a model that is nonlinear in its parameters and our difficulty in finding a stable external reference made both error estimates from local curvature of the χ^2 surface and/or from Monte Carlo simulations of the data difficult.

For some fraction of our ftSHG experiments (one experiment on hPPS and one on PPS particles) we found that there was relatively large (and physically implausible) variation in model parameters for the best fit solutions. Often in these cases the standard deviation of a particular parameter was larger than the value of the parameter itself. In general, these fitting difficulties occurred with experiments with relatively fewer data points than others. We therefore assumed that this large deviation in model

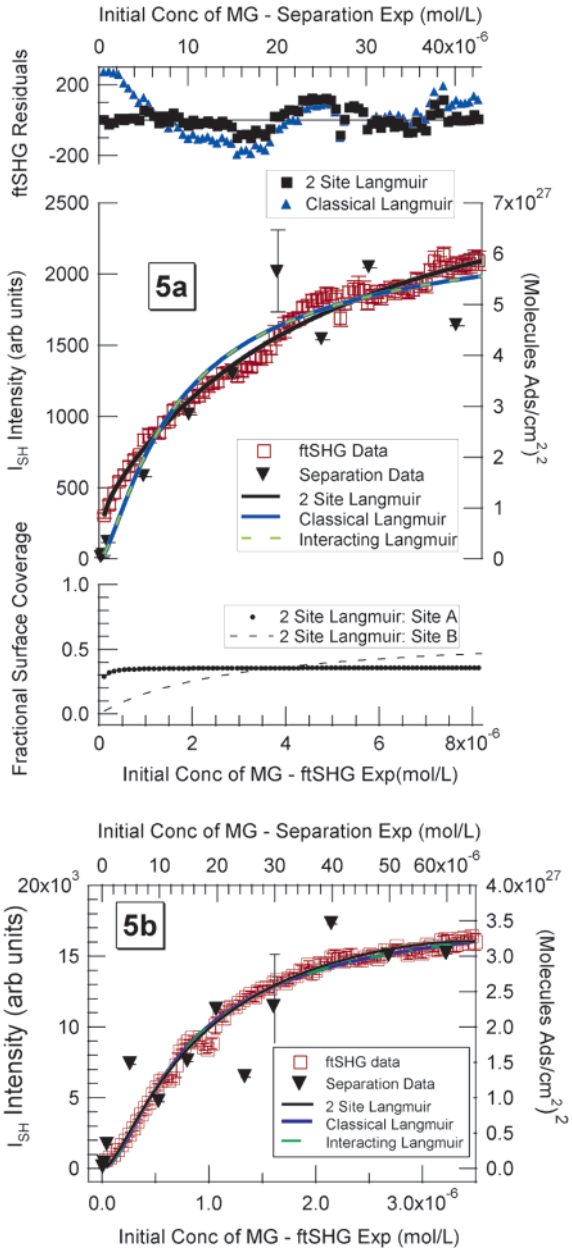

Figure 5. (a) Fits of simplified versions of the classical Langmuir, interacting Langmuir, and two-site Langmuir models to one of the ftSHG experiments describing adsorption of MG on cPPS particles and the corresponding data. Also shown is the square of the adsorbate density measured in one of the cPPS separation experiments, residuals of the fits of the two site and classical Langmuir models to the ftSHG data as well as the surface coverage of the individual sites in the two site model as a function of initial concentration of MG. (b) Fits of generalized versions of the classical Langmuir, interacting Langmuir, and two-site Langmuir models to one of the ftSHG MG adsorption on PPS experiments and the corresponding data. Also shown is the square of the adsorbate density measured in one of the MG on PPS separation experiments.

parameter values was caused by a lack of precision in the determination of χ^2_{red}, i.e., an undersampling of χ^2 space by the data, and did not consider these results further.

3. Results and Discussion

In general, we wish to answer two questions from these experiments. First, what is the best model for each particle type (in particular is there evidence that a two-site model offers a better description of MG adsorption at particle surfaces likely to have two adsorption sites)? Second, how precise is our knowledge of the parameters gleaned from this best model? The first question is addressed by calculating the χ^2_{red} of each model fit to all experiments and averaging the χ^2_{red} for all fits of a particular model to all experiments on a particular particle type.

Cursory inspection of these results, shown in Table 2, leads to several immediate observations. First, for ftSHG experiments on cPPS and hPPS particles there is no difference between generalized versions of our models and simplified versions that assume $[MG_{bulk}] \gg [MG_{surf}]$. This observation suggests that for these systems $[MG_{bulk}] \gg [MG_{surf}]$ and that application of the generalized models with the hope of gaining extra parameters is not appropriate. Second, it is clear that, to within one standard deviation in χ^2_{red}, the two-site model is a better description of the data than either the classical Langmuir or the interacting Langmuir for MG adsorption on cPPS and hPPS particles. The analysis of ftSHG measurements of MG adsorption on PPS particles leads to markedly different conclusions. For this system the generalized models appear to be consistently favored over the simplified models, arguing that in this case $[MG_{bulk}] \approx [MG_{surf}]$. In addition, for the MG on PPS system, it is clear that the classical Langmuir model offers the best description of the data. The model fits suggest that for the cPPS and the hPPS systems $[MG_{bulk}] \gg [MG_{surf}]$ while for the PPS system $[MG_{bulk}] \sim [MG_{surf}]$. This model result is internally consistent, on average the adsorption on PPS is more energetically favored. Prior studies of the MG on PPS system[41] have reported that, in a comparison between a generalized and a simplified Langmuir model, the generalized was superior, in agreement with our findings. However, in that work no attempt to quantify this difference was made.

The averaged χ^2_{red} values tabulated in Table 2 give us a quantitative measure of the goodness of fit to each type of model. We can see these differences qualitatively by comparing the fits of simplified versions of the model to a cPPS experiment (Figure 5a) and generalized versions of the models to a PPS experiment (Figure 5b). Comparing these two results highlights that the two-site model is a markedly better fit for the cPPS case over the entire concentration range (for fit residuals see Figure 5a) while all models appear to be equivalent for the PPS. One set of separation data for cPPS and one for PPS particles is also shown in Figure 5 for comparison purposes.

Our attempts to interpret our separation experiments are considerably less conclusive (Table 2). We expect to be able to determine χ^2_{red} less precisely, and therefore have less ability to distinguish between different surface models, for the separation experiments than the ftSHG for two reasons: generally the ftSHG experiments have 10× more data points and, while precise minimum error estimates for the ftSHG experiments are relatively straightforward, precise error estimates (of any kind) for the separation experiments are not. That said, it is clear that none of the simplified versions of our models describe MG adsorption on any particle for these experiments. We conclude from this result that $[MG_{bulk}]$ is of order $[MG_{surf}]$ for all separation experiments. For example, at 1 μM initial concentration of MG in both the cPPS and PPS systems (examples shown in Figure 5a and 5b) ~90% of the MG initially added to solution is adsorbed. Over the range of initial concentrations employed in both experiments the amount found on the surface is never less than 10% of that initially added. This difference between the ftSHG and separation experiments is consistent with the fact that the particle concentration used in the separation experiments was ~10× higher than that used in the ftSHG. Panels a and b of Figure 5 also show one separation experiment

TABLE 2: χ^2_{red} for Model Fits to SHG and Separation Experiments[a]

	Lang	gLang	iLang	giLang	2Lang	g2Lang
assumption	$[MG_{bulk}] \gg [MG_{surf}]$	NA	$[MG_{bulk}] \gg [MG_{surf}]$	NA	$[MG_{bulk}] \gg [MG_{surf}]$	NA
particle type (no. of exp)/exp type						
cPPS(3)/ftSHG	11.3 ± 5.2	11.4 ± 5.3	11.6 ± 5.3	11.6 ± 5.3	$\mathbf{1.6 \pm 0.8}$	1.6 ± 1.0
hPPS(2)/ftSHG	6.0 ± 0.1	6.0 ± 0.1	6.1 ± 1.1	6.1 ± 1.1	$\mathbf{2.5 \pm 0.3}$	2.5 ± 0.4
PPS(3)/ftSHG	18.1 ± 9.4	$\mathbf{6.9 \pm 0.3}$	15.0 ± 6.5	11.9 ± 7.6	18.5 ± 8.0	18.6 ± 10.2
cPPS(2)/sep	NA	26.2 ± 4.9	7800 ± 0.3	23.9 ± 4.2	NA	60.4 ± 66.7
hPPS(2)/sep	NA	2.0 ± 0.6	$2270 \pm 7\ 9$	4.8 ± 1.8	NA	3.3 ± 1.1
PPS(2)/sep	NA	1.4 ± 0.3	$863 \pm$ NA	1.02 ± 0.3	NA	27.5 ± 36.7

[a] Reported values are averages ± one standard deviation. NA on this table indicates experimental analyses for which no physically valid fit to the data could be found.

TABLE 3: Model Parameters for Fits to SHG Data[a]

particle type	ΔG_A, kJ/mol	ΔG_B, kJ/mol	N_{mA}/N_m, %	N_{mB}/N_m, %	N_m, sites/cm^2
hPPS	−43.7(−0.2/+0.3)	−54.6(±0.2)	84 ± 1	16 ± 1	NA
cPPS	−40.3(−0.8/+1.2)	−51.7(−0.9/+1.3)	65 ± 3	35 ± 3	NA
PPS	−48.8(−1.2/2.3)	NA	NA	NA	$5.4 \times 10^{13}(\pm 2.4 \times 10^{13})$

[a] NA on this table indicates parameters not applicable to the model that best describes the PPS data. PPS maximum adsorbate density as a function of surface area is calculated by multiplying the maximum adsorbate concentration, a model parameter, by the specific surface area of the suspension. The specific surface area is calculated from particle size information furnished by the manufacturer.

TABLE 4: N_m Inferred from Separation Experiments

particle type	N_m sites/cm^2
hPPS	$5.9 \times 10^{13}(\pm 2.5 \times 10^{13})$
cPPS	$6.8 \times 10^{13}(\pm 1.4 \times 10^{13})$
PPS	$4.0 \times 10^{13}(\pm 2.7 \times 10^{13})$

on cPPS and PPS particles, respectively. While no fits to these data are shown in the figures, it is clear by inspection that the ability to justify the application of the two-site model to the cPPS particles would require many more data points than collected in the typical separation experiment.

Having determined the models providing the best fits to the ftSHG generated isotherms we proceeded to examine the model parameters generated from each of the fits (Table 3). Inspection of these model parameters suggests several characteristics for the MG on hPPS and cPPS systems. First, fits to multiple experiments produce site energies that are statistically distinguishable (i.e., the error bars on the quantities in Table 3 do not overlap). Second, site energies resulting from the two-site fits are also physically distinguishable: the difference between the site energies for a given particle type is significantly greater than thermal energy (kT). For example, for MG adsorption on cPPS $\Delta G_{ads} = -40.3$ and -51.7 kJ/mol for sites A and B, respectively. By comparison kT under these conditions is 2.4 kJ/mol. For the experiments on PPS particles we calculated a single surface energy of -48.8 kJ/mol and a site density of 5.4×10^{13} molecules/cm^2. Both the site energy and density differ from previous studies of this system, Wang et al.[21] and Eckenrode et al.[23] at pH 4, which found -51.8 kJ/mol and 2.6×10^{13} molecules/cm^2 and -51.7 kJ/mol and 3.71×10^{13} molecules/cm^2 respectively. In general these differences fall within experimental error but it is worth noting that both particle surface characteristics and MG protonation state are expected to differ as a function of pH and these changes may contribute to the observed differences.

It is possible to rationalize the conclusion that there are two kinds of adsorption sites for the cPPS and hPPS particles and only one kind of site on the PPS particles based on what is known about the bulk chemistry of each particle type. As described by the manufacturer, all particles contain trace amounts of sulfonate-containing surfactant and the hPPS and cPPS particles are formed by a combination of polystyrene and a polymer rich in the desired functional group. While the surface concentration of each species has not been measured, the bulk concentration of carboxyl and hydroxyl groups (in cPPS or hPPS particles) is 5−10 mmol/L while the concentration of sulfontate groups (in cPPS, hPPS, and PPS particles) is 2.5−5 μmol/ L.[42] The significantly lower bulk sulfonate concentration suggests that there may simply not be enough sulfonate groups at the PPS particle surface for such sites to be quantitatively important in describing MG adsorption. If this is true then it argues that adsorption of MG on PPS particles likely occurs only at phenyl groups while adsorption on hPPS/cPPS particles occurs at hydroxyl/carboxyl groups in addition to phenyl groups. We expect that the adsorption energy of MG at phenyl groups might be different at different particle surfaces (because the orientation and packing density of phenyls may change with molecular environment[43]). However, it seems reasonable to suggest that the variability in MG adsorption energy at phenyl groups be less than the variability in MG adsorption energy at carboxyl/hydroxyl groups. If this is the case the type B sites on cPPS and hPPS particles are likely phenyl groups while the A sites are the hydroxyl or carboxyl groups. It is worth noting that there are other possible means of rationalizing our model results. We have shown only that for cPPS and hPPS particles a surface model with two noninteracting sites better explains MG adsorption data than a model with one site or a model with one site and adsorbate−adsorbate interaction. On the basis of the synthetic procedure used in fabrication of these colloids it seems most likely that these two sites reflect surface chemical functional group heterogeneity.

Our results are, however, also consistent with a more complicated scenario in which multilayer adsorption occurs on cPPS and hPPS (where the second adsorption site is adsorption of MG on MG) but not on PPS particles. For such multilayer adsorption to be consistent with our data adsorbate molecules in the first and second layer would have to be similarly oriented relative to the surface, otherwise some decrease in I_{SH} (such as for binary mixtures of acetone and water[36]) would be expected at high $[MG_{bulk}]$, and ΔG_{ads} for adsorption of MG on MG would have to be relatively similar to that of MG on polystyrene, otherwise our results would more closely resemble the Type B isotherm in Figure 4. Given our knowledge of the colloid

TABLE 5: Site Densities of MG Adsorption[a]

particle type	N_{mA}, sites/cm^2	N_{mB}, sites/cm^2
hPPS	$5.0 \times 10^{13}(\pm 2.1 \times 10^{13})$	$9.4 \times 10^{12}(\pm 4.0 \times 10^{12})$
cPPS	$4.4 \times 10^{13}(\pm 9.1 \times 10^{12})$	$2.4 \times 10^{13}(\pm 4.9 \times 10^{12})$
particle type	$N_{m,SHG}$, sites/cm^2	$N_{m,SEP}$, sites/cm^2
PPS	$5.4 \times 10^{13}(\pm 2.4 \times 10^{13})$	$4.0 \times 10^{13}(\pm 2.7 \times 10^{13})$

[a] For PPS particles $N_{m,SHG}$ indicates the site density calculated from the SHG experiments while $N_{m,SEP}$ indicates that measured in the separation.

synthesis (in particular the fact that the functionalized latex particles are a mixture of polystyrene and some other functional group bearing polymer) the relatively simpler conclusion of surface chemical functional group heterogeneity (and monolayer adsorption of MG) seems substantially more likely. As discussed earlier our results may also be consistent with more complicated surface models: principally one- or two-site models that assign a distribution (of varying complexity) of site energies to each adsorption site. In reality adsorption is likely characterized by such a distribution of energies for chemically identical sites (one possible mechanism might be a distribution in orientation of particle surface functional groups[43]). However, we did not attempt to use such models in describing our data for two reasons. First we wanted to limit the number of free parameters for each of the fits to data as much as possible to facilitate the ability to resolve χ^2_{red} differences between models. Second, for a distribution of site energies to influence our qualitative conclusions (e.g., cause us to mistake two-site adsorption for one) the distribution of adsorption energies for a single functional group would have to be of order of the difference in adsorption energies for chemically different functional groups. This scenario seemed unlikely.

If our tentative identification of each of the surface sites on this particle is accurate, then the relative site densities for each particle type are an indicator of the relative amount of each polymer at the particle surface, and give insight into the effectiveness of the particle synthesis in imparting surface functionality. However, placing limits on the ability to functionalize these particles by the attachment of other molecules to carboxyl or hydoxyl groups requires that we actually quantify the density of these groups at the surface. As discussed above for the ftSHG experiments, $[MG_{bulk}] \gg [MG_{surf}]$. In this situation the generalized two-site Langmuir model reduces to its simplified version and we can only estimate relative amounts of the two sites. To quantify site densities on the hPPS and cPPS particles requires use of the separation data.

Cursory inspection of Table 2 suggests that it is impossible to choose a best model for description of data from the separation experiments (i.e., given the error estimates for χ^2_{red} we cannot distinguish the best fitting model for any of the three experimental systems). However, the parameter N_m, the total number of molecules on the surface at saturation, appears in each of the model treatments of the separation experiments. We therefore averaged the N_m from the generalized models and report these data in Table 4. Put another way, we have assumed that the N_m calculated in each generalized model is equally valid (recall that for the separation experiment no single model stood out as providing the best fit to the data), and that the deviation of each of these estimates from the true value of N_m is random. To within our measurement precision the density of surface sites on each particle type is the same. Knowing N_m (total number of surface sites) for the hPPS and cPPS particles we can calculate the density of each type of surface group (Table 5). This information is of use should one desire to functionalize these particles. For instance, in an application requiring the attaching of a polypeptide via an amide bond to a carboxyl group, 4.4×10^{13} molecules/cm^2 would be the maximum attachment density attainable on cPPS. The N_m for MG adsorbed on PPS particles was already obtained by model fit to the ftSHG data and agrees with the N_m measured from the separation experiments to within the estimated precision.

Prior work describing the adsorption of MG on PPS, sulfonated PPS, and aminated PPS particles observed a trend in adsorption energies that could be rationalized by electrostatic arguments: adsorption of cationic MG on nominally negative sulfonated PPS particles was most favorable, followed by adsorption on neutral, i.e., PPS, and positively charged particles, i.e., aminated PPS.[23] We observed no such trend in our results: cPPS particles are expected to be nominally negative while PPS and hPPS are both expected to be neutral. The differences between the studies may possibly be explained by the different pH we employed (pH 3 to 4) but may also be a function of the model chosen to describe the surface: Eckenrode et al.[23] used a single-site, generalized Langmuir model to extract surface characteristics from isotherms describing MG adsorption on sulfonated and aminated PPS particles. On the basis of the results presented here it may be worthwhile to revisit that analysis for these relatively complex surfaces.

4. Conclusion

Colloids in aqueous suspension are of interest to a variety of fundamental and applied problems and often have chemically heterogeneous surfaces. This heterogeneity often makes it difficult to understand adsorption at colloid surfaces as it provides multiple mechanisms by which even physisorption might occur. While it is thus important to quantify the relative density and adsorption energies of multiple adsorption sites on the colloid surface, this measurement is difficult. Here we demonstrate that with the creation of high resolution adsorption isotherms this information can be inferred with relatively high precision from relatively simple measurements.

We here create adsorption isotherms of the MG/latex particle system using the ftSHG and separation techniques. The ftSHG technique differs from the separation technique principally in allowing the collection of isotherms with many data points due to the ability to automate both sample creation and measurement. In addition, because of the inherent surface sensitivity of SHG, the ftSHG technique may be used to create isotherms of relatively sparse surface species. We find that our ftSHG isotherms allow us to quantitatively distinguish between the appropriateness of several different surface models. This type of analysis is not possible for our, and virtually all, isotherms generated by using conventional, separation techniques.

After determination of the best fitting model we find, in agreement with our expectations, that PPS particles have one adsorption site (probably surface phenyl groups) while cPPS and hPPS particles have two (most likely surface carboxyl and hydroxyl groups, respectively, in addition to the phenyls). We expect these site densities (see Table 5) to be of use to those interested in efficiently functionalizing these particles for biotechnology applications. This study also suggests that it may be useful, when possible, to conduct ftSHG and separation experiments in parallel: that the methods provide complementary information.

Acknowledgment. The authors gratefully acknowledge the experimental assistance of Ali Eftekhari, the support of the donors of the American Chemical Society Petroleum Research

Fund, and the support of the National Science Foundation (NSF) of the U.S. through grant CHE-0089156 (Molecular level analysis of macromolecule-surface interactions in bacterial adhesion). During the course of this work R.K.C. was supported by the Pennsylvania State University Biogeochemical Research Initiative for Education (BRIE), which was partially supported through NSF grant DGE (IGERT)-9972759 as well as an NSF East Asian and Pacific Summer Institute Fellowship. H.F.W. acknowledges the generous support of the Natural Science Foundation of China (NSFC, No. 20425309) and the Chinese Ministry of Science and Technology (MOST, No. G1999075305).

References and Notes

(1) Ben-Dan, T.; Wynne, D.; Shteinman, B.; Hu, Z.; Kamenir, Y. *Water Sci. Technol.* **2000**, *42*, 49−54.
(2) West, J.; Halas, N. *Annu. Rev. Biomed. Eng.* **2003**, *5*, 285−292.
(3) Cvetkovic, V.; Painter, S.; Turner, D.; Pickett, D.; Bertetti, P. *Water Resour. Res.* **2004**, *40*, art. no. W06504.
(4) Bekhit, H.; Hassan, A. *Water Resour. Res.* **2005**, *41*, art. no. W02010.
(5) Somorjai, G. A. *Introduction to Surface Chemistry and Catalysis*; John Wiley and Sons: New York, 1994.
(6) Camesano, T. A.; Wilkinson, K. J. *Biomacromolecules* **2001**, *2*, 1184−1191.
(7) Lacava, B. M.; Azevedo, R. B.; Silva, L. P.; Lacava, Z. G. M.; Neto, K. S.; Buske, N.; Bakuzis, A. F.; Morais, P. C. *Appl. Phys. Lett.* **2000**, *77*, 1876−1878.
(8) Turov, V. V.; Leboda, R.; Bogillo, V. I.; Skubiszewska-Zieba, J. *Langmuir* **1997**, *13*, 1237−1244.
(9) Tejedor-Tejedor, M. I.; Yost, E. C.; Anderson, M. A. *Langmuir* **1990**, *6*, 979−987.
(10) Franzen, S.; Folmer, J. C. W.; Glomm, W. R.; O'Neal, R. *J. Phys. Chem. A* **2002**, *106*, 6533−6540.
(11) Chitrakar, R.; Tezuka, S.; Sonoda, A.; Sakane, K.; Ooi, K.; Hirotsu, T. *J. Colloid Interface Sci.* **2005**, *290*, 45−51.
(12) Peacock, C. L.; Sherman, D. M. *Geochim. Cosmochim. Acta* **2004**, *68*, 2623−2637.
(13) Peacock, C. L.; Sherman, D. M. *Geochim. Cosmochim. Acta* **2005**, *69*, 3733−3745.
(14) Shen, Y. *Annu. Rev. Phys. Chem.* **1989**, *40*, 327−350.
(15) Heinz, T. F. In *Nonlinear Surface Electromagnetic Phenomenon*; Ponath, H.-E., Stegeman, G. I., Eds.; Elsevier Science Publishers: New York, 1991.
(16) Corn, R. M.; Higgins, D. A. *Chem. Rev.* **1994**, *94*, 107−125.
(17) Eisenthal, K. B. *Chem. Rev.* **1996**, *96*, 1343−1360.
(18) Wang, H.; Yan, E. C. Y.; Borguet, E.; Eisenthal, K. B. *Chem. Phys. Lett.* **1996**, *259*, 15−20.
(19) Yan, E. C. Y.; Eisenthal, K. B. *Biophys. J.* **2000**, *79*, 898−903.
(20) Yan, E. C. Y.; Eisenthal, K. B. *J. Phys. Chem. B* **2000**, *104*, 6686−6689.
(21) Wang, H. F.; Troxler, T.; Yeh, A. G.; Dai, H. L. *Langmuir* **2000**, *16*, 2475−2481.
(22) Eckenrode, H. M.; Dai, H. L. *Langmuir* **2004**, *20*, 9202−9209.
(23) Eckenrode, H. M.; Jen, S. H.; Han, J.; Yeh, A. G.; Dai, H. L. *J. Phys. Chem. B* **2005**, *109*, 4646−4653.
(24) Yan, E. C. Y.; Liu, Y.; Eisenthal, K. B. *J. Phys. Chem. B* **1998**, *102*, 6331−6336.
(25) Jackler, G.; Wittemann, A.; Ballauff, M.; Czeslik, C. *Spectroscopy* (*Amsterdam, Neth.*) **2004**, *18*, 289−299.
(26) Wittemann, A.; Ballauff, M. *Macromol. Biosci.* **2005**, *5*, 13−20.
(27) Kawaguchi, H. *Prog. Polym. Sci.* **2000**, *25*, 1171−1210.
(28) Personal communication with Polysciences, Inc., 2005.
(29) Rao, Y.; Tao, Y. S.; Wang, H. F. *J. Chem. Phys.* **2003**, *119*, 5226−5236.
(30) Schiebener, P.; Straub, J.; Sengers, J. M. H. L.; Gallagher, J. S. *J. Phys. Chem. Ref. Data* **1990**, *19*, 677−717.
(31) Ma, X. Y.; Lu, J. Q.; Brock, R. S.; Jacobs, K. M.; Yang, P.; Hu, X. H. *Phys. Med. Biol.* **2003**, *48*, 4165−4172.
(32) Yao, H.; Inoue, Y.; Ikeda, H.; Nakatani, K.; Kim, H. B.; Kitamura, N. *J. Phys. Chem.* **1996**, *100*, 1494−1497.
(33) Kikteva, T.; Star, D.; Leach, G. W. *J. Phys. Chem. B* **2000**, *104*, 2860−2867.
(34) Simpson, G. J.; Rowlen, K. L. *Anal. Chem.* **2000**, *72*, 3399−3406.
(35) Simpson, G. J.; Rowlen, K. L. *Anal. Chem.* **2000**, *72*, 3407−3411.
(36) Chen, H.; Gan, W.; Wu, B.-h.; Wu, D.; Guo, Y.; Wang, H.-f. *J. Phys. Chem. B* **2005**, *109*, 8053−8063.
(37) Chen, H.; Gan, W.; Lu, R.; Guo, Y.; Wang, H.-f. *J. Phys. Chem. B* **2005**, *109*, 8064−8075.
(38) Ong, S.; Zhao, X.; Eisenthal, K. B. *Chem. Phys. Lett.* **1992**, *191*, 327−335.
(39) Taylor, J. R. *An Introduction to Error Analysis*: *The Study of Uncertainties in Physical Measurements*; University Science Books: Mill Valley, CA, 1982.
(40) Yang, N.; Angerer, W. E.; Yodh, A. G. *Phys. Rev. Lett.* **2001**, *8710*, art. no. 103902.
(41) Wang, H.-f.; Yan, E. C. Y.; Liu, Y.; Eisenthal, K. B. *J. Phys. Chem. B* **1998**, *102*, 4446−4450.
(42) Personal communication with Polysciences, Inc. Data are for 6 μm particles; however, the synthesis protocol used to generate the 1 μm particles we used is not significantly different, 2005.
(43) Yang, C. S. C.; Wilson, P. T.; Richter, L. J. *Macromolecules* **2004**, *37*, 7742−7746.
(44) Adamson, A. W. *Physical Chemistry of Surfaces*; Wiley: New York, 1990.
(45) Turro, N. J.; Lei, X.-G.; Li, W.; Liu, Z.; McDermott, A.; Ottaviani, M. F.; Abrams, L. *J. Am. Chem. Soc.* **2000**, *122*, 11649−11659.